HAL
archives-ouvertes.fr

Peregrine soliton generation and breakup in standard telecommunications fiber

Kamal Hammani, Bertrand Kibler, Christophe Finot, Philippe Morin, Julien Fatome, John Dudley, Guy Millot

▶ **To cite this version:**

Kamal Hammani, Bertrand Kibler, Christophe Finot, Philippe Morin, Julien Fatome, et al.. Peregrine soliton generation and breakup in standard telecommunications fiber. Optics Letters, Optical Society of America, 2011, 36 (2), pp.112-114. <10.1364/OL.36.000112>. <hal-00542997>

HAL Id: hal-00542997
https://hal.archives-ouvertes.fr/hal-00542997

Submitted on 5 Dec 2010

HAL is a multi-disciplinary open access archive for the deposit and dissemination of scientific research documents, whether they are published or not. The documents may come from teaching and research institutions in France or abroad, or from public or private research centers.

L'archive ouverte pluridisciplinaire **HAL**, est destinée au dépôt et à la diffusion de documents scientifiques de niveau recherche, publiés ou non, émanant des établissements d'enseignement et de recherche français ou étrangers, des laboratoires publics ou privés.

Peregrine soliton generation and breakup in standard telecommunications fiber

Kamal Hammani,[1] Bertrand Kibler,[1*] Christophe Finot,[1]

Philippe Morin,[1] Julien Fatome,[1] John M. Dudley[2] and Guy Millot[1]

[1]Laboratoire Interdisciplinaire Carnot de Bourgogne, UMR 5209 CNRS/Université de Bourgogne, 21078 Dijon, France
[2] Institut Femto-ST, UMR 6174 CNRS/Université de Franche-Comté, 25030 Besançon, France
[*]Corresponding author: bertrand.kibler@u-bourgogne.fr

We present experimental and numerical results showing the generation and breakup of the Peregrine soliton in standard telecommunications fiber. The impact of non-ideal initial conditions is studied through direct cut back measurements of the longitudinal evolution of the emerging soliton dynamics, and is shown to be associated with the splitting of the Peregrine soliton into two subpulses, with each subpulse itself exhibiting Peregrine soliton characteristics. Experimental results are in good agreement with simulations.

OCIS codes: 060.4370 (Nonlinear optics, fibers), 060.5530 (Pulse propagation and temporal solitons),

There is currently much research interest into extreme-value fluctuations and "optical rogue wave" localization processes in nonlinear fiber optics and supercontinuum generation [1-2]. These results have motivated a number of studies into the initial dynamics of the supercontinuum generation process, and it was shown in particular that the temporal and spectral characteristics of the evolving field could be well described in terms of a particular class of nonlinear Akhmediev breather (AB) structure that undergoes periodic evolution with propagation and periodic energy exchange with a finite background [3]. AB characteristics are observed when a weakly-modulated continuous wave is injected in the anomalous dispersion regime of an optical fiber, and can be described in terms of an analytic solution of the nonlinear Schrodinger equation (NLSE) given by [4-6].

$$A(z,T) = \sqrt{P_0}\ \frac{(1-4a)\cosh(bz/L_{NL}) + ib\sinh(bz/L_{NL}) + \sqrt{2a}\cos(\omega_{\mathrm{mod}}T)}{\sqrt{2a}\cos(\omega_{\mathrm{mod}}T) - \cosh(bz/L_{NL})}. \qquad (1)$$

Here, $A(z,T)$ is the field envelope, and the injected field has average power P_0 and is modulated at frequency ω_{mod}. Breather dynamics are observed for frequencies experiencing modulation instability gain, corresponding to $0 < a < 1/2$ with $2a = [1-(\omega_{\mathrm{mod}}/\omega_c)^2]$ and $\omega_c^2 = 4\,\gamma P_0/|\beta_2|$. Here γ and β_2 refer to the fiber nonlinearity and dispersion, the nonlinear length is $L_{NL} = (\gamma P_0)^{-1}$ and the parameter $b = [8a\,(1-2a)]^{1/2}$ determines the instability growth. The asymptotic case $a \rightarrow 1/2$ is known as the Peregrine soliton (PS), and is of particular interest as it represents the analytical limit of a wide class of NLSE solutions and because it has the rational form: $A(z,T) = \sqrt{P_0}\ [1-4(1+2iz/L_{NL})/(1+4(T/T_0)^2+4(z/L_{NL})^2]\exp(iz/L_{NL})$ where $T_0 = (\beta_2 L_{NL})^{1/2}$.

Despite its existence in the mathematical literature for over 25 years, the PS solution has only very recently been observed in experiments. Two narrow-linewidth lasers were used to generate initial conditions to excite PS localization in highly nonlinear fiber characterized using intensity and phase measurements with frequency-resolved optical gating [7].

In this Letter, we further explore the generation of PS characteristics in fibers, using a much simplified setup that allow us to study the evolution dynamics over a wider range of initial conditions. The setup is shown in Fig. 1 and is based exclusively on commercially-available telecommunication-ready components and standard silica SMF-28 fiber. In contrast to previous experiments using combined external cavity lasers to create an amplitude modulated beat signal, we use a simpler approach here with a directly intensity modulated 1550 nm laser diode, and an ultrafast optical sampling oscilloscope (OSO – Picosolve PSO100 series) that enables real time observation of the temporal reshaping towards the PS. We also perform high dynamic range spectral characterization, and note that a phase modulator is used to prevent from the deleterious consequences of Brillouin scattering, and an erbium-doped fiber amplifier (EDFA) is used to obtain average powers up to 1W. The optical fiber is an 8.35-km long segment of SMF-28 with β_2 = -21.4 ps^2/km, β_3 = 0.12 ps^3/km, γ = 1.2 W^{-1}/km^{-1} and 0.19 dB/km loss. The output signal is carefully characterized both in the temporal and spectral domains by means of an optical spectrum analyzer and an optical sampling oscilloscope that enables the direct measurement of the (subpicosecond) intensity profile in real-time. By combining the real time characterization with cut-back measurements, we provide the first direct observation of PS longitudinal evolution dynamics and report a new effect associated with the breakup of a PS into two subpulses, each possessing similar characteristics of localization upon finite background.

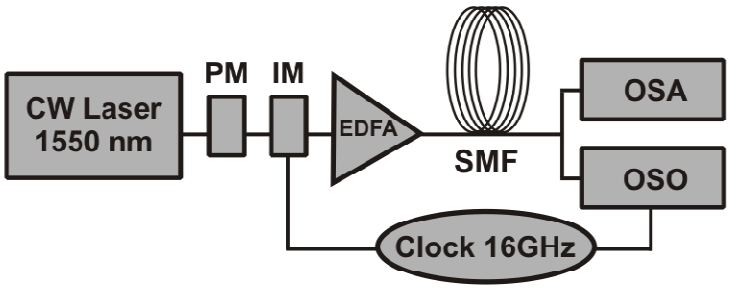

Fig. 1: Experimental setup. PM: phase modulator, IM: intensity modulator, OSO: optical sampling oscilloscope; OSA: optical spectrum analyzer.

The field injected into the fiber is $A(z=0,T)=\sqrt{P_0}\left[1+\delta_{\mathrm{mod}}\cos\left(\omega_{\mathrm{mod}}T\right)\right]^{1/2}$, where δ_{mod} is the intensity modulation contrast. As this modulated field propagates along the fiber, it undergoes dynamical nonlinear compression to yield pulses that grow to high amplitude before returning to the initial state through Fermi-Pasta-Ulam recurrence. Our present setup is very convenient to study the precise impact of the initial conditions on this evolution. Indeed, we performed temporal and spectral characterization at $\omega_{\mathrm{mod}}/2\pi$ = 16 GHz using different values of δ_{mod} in the range 0.2–0.6 and twelve values of power P_0 from 0.35 to 0.9 W. The power range in particular enables us to study the dynamics over an extended region of the gain curve from $0.4 < a < 0.47$, allowing us to approach much closer the ideal PS limit than in previous experiments performed at a = 0.42 [7]. Moreover, the longitudinal evolution of the field was studied by cutting the fiber in 32 parts.

The first results we present in Fig. 2 concern the propagation dynamics as a function of power and distance. At fixed modulation contrast δ_{mod} = 0.3, Fig. 2(a) illustrates how the degree of dynamical compression strongly depends on initial conditions by plotting the compressed

pulse peak power as a function of propagation distance for powers in the range 0.35–0.9 W. The peak power was determined from average power measurements and the measured OSO temporal profiles. The results are shown in false-color representation clearly illustrating how the distance of optimum compression decreases at higher powers. The experimental results are compared with numerical simulations shown in Fig. 2(b). At the highest powers, the simulations also show the appearance of a secondary compression phase; in fact we study this in more detail in Fig. 3 where we show it is associated with a pulse splitting effect.

The PS propagation dynamics are known to depend sensitively on the initial modulation depth. Indeed, the ideal evolution towards the PS is expected to occur for smaller values of δ_{mod} with evolution over a longer propagation distance [3]. For fixed input power $P_0 = 0.80$ W, Fig. 2(c) presents results for three values of $\delta_{mod} = 0.2, 0.3, 0.4$ where we plot the temporal intensity profile measured at the distance of optimum compression L = 7.3, 4.6, 4.2 km, respectively. We clearly see that lower δ_{mod} requires longer propagation distances for optimal compression, but our ability to readily characterize the evolution for these different cases allows us to see that greater propagation distance associated with the lowest δ_{mod} results in deviation from the ideal PS characteristics because of significant loss. From our results, the best agreement with the expected PS structure is at $\delta_{mod} = 0.3$ where we see a clear temporally localized peak surrounded by a non-zero background. The central part of the structure has a temporal duration around 3 ps and closely follows the analytical formula as well as the numerical simulations based on the extended NLSE taking into account third order dispersion, losses, Raman effects and ASE noise at the experimental level. The excellent agreement observed in the temporal domain is also confirmed in the spectral domain as illustrated in Fig. 2(d).

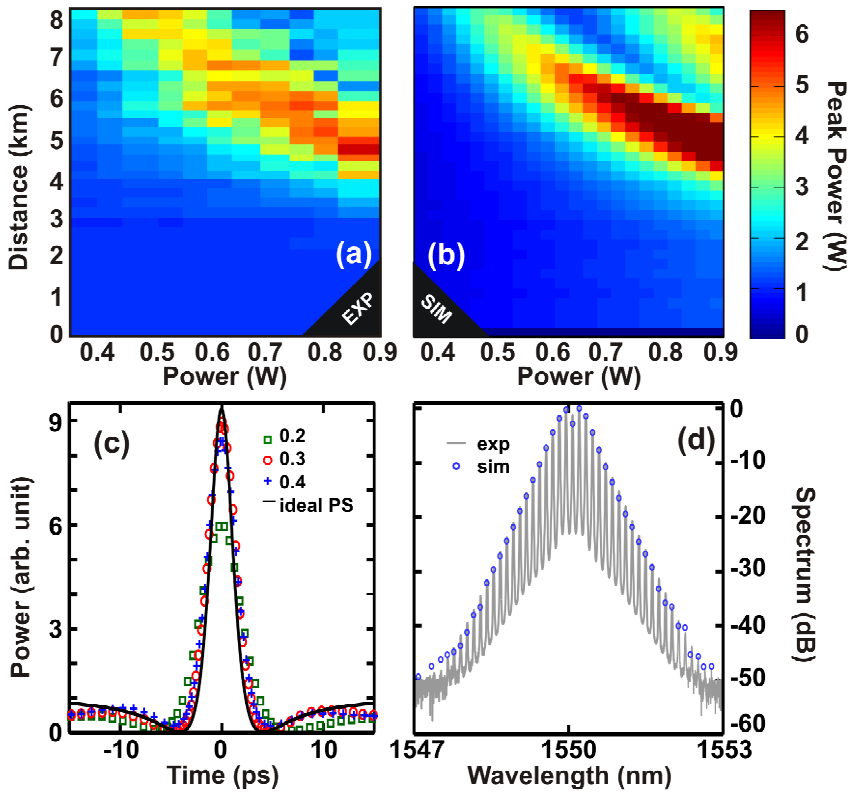

Fig. 2: False color maps showing compressed peak power as a function of distance and power at δ_{mod}=0.3 from: (a) experiment and (b) simulation. (c) Comparison of the temporal intensity profile measured for three values of δ_{mod} at corresponding optimum compression distance with P_0=0.8W (see details in the text). The ideal analytic PS is also shown in black line. Corresponding numerical simulations of δ_{mod}=0.3 yield results that are indistinguishable from the experimental data. (d) Corresponding spectrum (solid grey line) at maximum compression for δ_{mod}=0.3 compared with numerical results (blue circles).

We now focus in more detail on the whole longitudinal evolution of the field corresponding to the results in Fig. 2 (c) and (d) when $\delta_{mod} = 0.3$ and $P_0 = 0.80$ W (i.e $a = 0.47$). Fig. 3 shows the longitudinal evolution of the temporal and spectral profiles obtained from experiment (a,c) and numerical simulations (b,d). We clearly observe the temporal evolution of the modulated CW field into a periodic train of ultrashort pulses on a continuous background, accompanied by a significant spectral broadening. Experiments and simulations are in excellent agreement, but significantly differ after the point of optimal compression. We do not observe the expected return to the initial state, but rather a new and striking effect of Peregrine soliton breakup into two identical structures. Corresponding temporal and spectral signatures of these dynamics can also be seen in Fig. 3(e,f).

The deviation from recurrent dynamics is attributed to the sensitivity of the propagation to non-ideal initial conditions as we approach the PS limit at higher values of a [4]. We stress that this behavior was not observed in previous experiments when lower values of a and more restricted propagation were used [7], and thus these results represent a significant new observation. In fact, our ability to readily characterize the temporal profiles using the OSO allows us to further see that the sub-pulses are each themselves very well-fitted by the analytical form of the ideal PS; comparison with the ideal PS for each sub-pulse is shown in Fig. 3(e) using $P_0 = 0.32$ W equal to the continuous background around the doublet pulses. This suggests that the Peregrine soliton profile represents an attractive structure after breakup processes, similar to behavior of the more well-known hyperbolic secant solitons of the NLSE. However, further theoretical work will be needed to determine the precise conditions under which such breakup is

initiated [8]. In particular, a recent study has reported specific conditions for which FPU recurrence can be affected by frequency doubling dynamics [9].

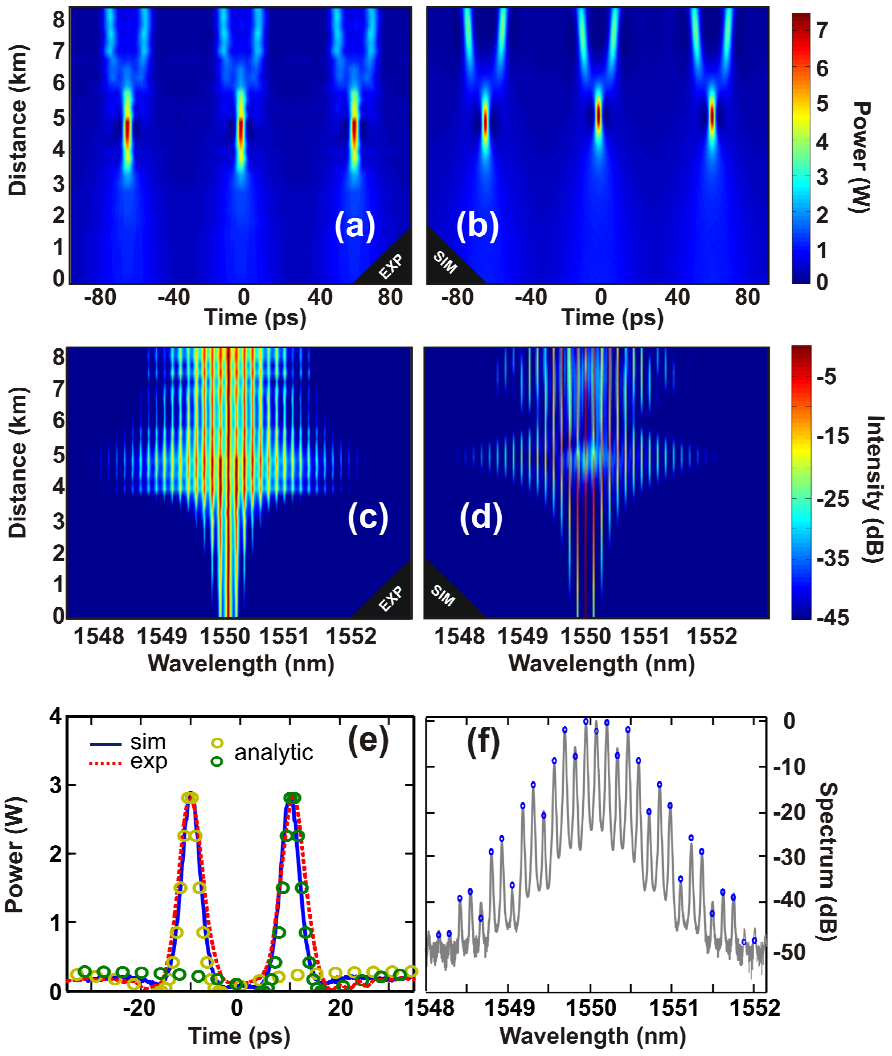

Fig. 3: Evolution with distance of temporal (a, b) and spectral (c, d) intensities comparing experiment and simulation as shown. Here δ_{mod} = 0.3 and P_0 = 0.80 W. (e) OSO signal observed at 8.4 km with δ_{mod} = 0.3. Experiment (dashed red line) is compared with simulations (solid blue line) and the analytical form of PS for each subpulse (yellow and green circles). (f) Corresponding spectrum with solid grey line compared with numerical spectrum (blue circles).

There are several conclusions to be drawn from this work. Firstly, we have shown that it is possible to generate near-ideal Peregrine soliton localization and to characterize the associated dynamics using a simple experimental setup with standard telecommunications components and measurement techniques. This allows the evolution of an initially modulated field towards the Peregrine soliton to be studied in a parameter limit very closely approaching the ideal theoretical limit, and furthermore permits the convenient and direct characterization of the propagation dynamics through cut-back measurements. These experiments reveal new features of this class of two-dimensional localization dynamics, including the sensitivity of the optimally-compressed profile on modulation depth, and a phenomenon of pulse breakup as the expected FPU recurrence is not observed with our experimental parameters. We anticipate that these results will impact on studies of the emergence of extreme localized events in optics under various initial excitation conditions. In a wider context, the fact that an initial Peregrine soliton can break up into two lower amplitude but equally strongly localized soliton pulses may have important implications for further interpretations of hydrodynamic rogue wave observations [10].

This work was supported by the Agence Nationale de la Recherche (ANR MANUREVA project: ANR-08-SYSC-019) and by the Conseil Régional de Bourgogne.

References

1. D. R. Solli, C. Ropers, P. Koonath, and B. Jalali, "Optical rogue waves," Nature **450**, 1054-1057 (2007).
2. J. M. Dudley, C. Finot, G. Millot, J. Garnier, G. Genty, D. Agafontsev, and F. Dias, "Extreme events in optics: Challenges of the MANUREVA project," Eur. Phys. J. Special Topics **185**, 125-133 (2010).
3. J. M. Dudley, G. Genty, F. Dias, B. Kibler, and N. Akhmediev, "Modulation instability, Akhmediev Breathers and continuous wave supercontinuum generation," Opt. Express **17**, 21497-21508 (2009).
4. N. Akhmediev and V. I. Korneev, "Modulation instability and periodic solutions of the nonlinear Schrödinger equation," Theor. Math. Phys. **69**, 1089–1093 (1986).
5. K. B. Dysthe and K. Trulsen, "Note on breather type solutions of the NLS as models for freak-waves," Phys. Scripta **T82** 48-52 (1999).
6. N. Akhmediev, A. Ankiewicz, and M. Taki, "Waves that appear from nowhere and disappear without a trace," Physics Letters A **373**, 675-678 (2009).
7. B. Kibler, J. Fatome, C. Finot, G. Millot, F. Dias, G. Genty, N. Akhmediev, and J. M. Dudley, "The Peregrine soliton in nonlinear fibre optics," Nature Phys. **6** , 790–795 (2010).
8. Y. Kodama and A. Hasegawa, "Nonlinear pulse propagation in a monomode dielectric guide," IEEE J. Quantum Electron. QE-**23**, 510–524 (1987).
9. S. Wabnitz and N. Akhmediev, "Efficient modulation frequency doubling by induced modulation instability," Optics Commun. **283**, 1152-1154 (2010).
10. V. I. Shrira and V. V. Geogjaev, "What makes the Peregrine soliton so special as a prototype of freak waves?," J. Eng. Mat. **67**, 11-22 (2010).